Supplementary Information

Surface fluorination of reactive battery anode materials for enhanced stability

Jie Zhao[†,⊥], Lei Liao[†,⊥], Feifei Shi[†], Ting Lei[‡], Guangxu Chen[†], Allen Pei[†], Jie Sun[†], Kai Yan[†], Guangmin Zhou[†], Jin Xie[†], Chong Liu[†], Yuzhang Li[†], Zheng Liang[†], Zhenan Bao[‡], and Yi Cui[†,§]*

[†]Department of Materials Science and Engineering, Stanford University, Stanford, California 94305, USA.

[‡]Department of Chemical Engineering, Stanford University, California 94305, USA.

[§]Stanford Institute for Materials and Energy Sciences, SLAC National Accelerator Laboratory, 2575 Sand Hill Road, Menlo Park, CA 94025, USA.

[⊥]These authors contributed equally.

Correspondence and requests for materials should be addressed to Y.C. (*email: yicui@stanford.edu).

Experimental methods

Fabrication of LiF-coated Li metal and LiF-Li$_x$Si NPs. 100 µL CYTOP (CTL-809 M from Asahi Glass Co.) was drop cast on the stainless-steel foil and dried at 120 ºC overnight in the argon glovebox (O$_2$ level < 0.1 ppm and H$_2$O level < 0.01 ppm). After drying, the stainless-steel foil with the polymer was placed at the bottom of the fluorination reactor (Schematic of the fluorination reactors, Figure S1). Li foil was polished mechanically to remove the native oxide, cut into four circular pieces with the diameter of 1 cm, and then instantly transferred into the reactor. The fluorination reactor was sealed and the polymer was heated at 350 ºC. During fluorination reaction, the fluorination reactor was placed in the argon glovebox. The temperature of the surface reaction with Li metal is controlled by the distance to the bottom of the reactor, which is measured to be 175 ºC. The fluorination time for Li metal is 12 h. Li$_x$Si NPs were synthesized by heating the mixture of Si NPs (500 mg, 100 nm, MTI, Inc) and Li foil (550 mg, Alfa Aesar) at 250 ºC under mechanical stirring at 200 rpm for 2 days in the argon glove box. 200 µL CYTOP was dried and placed at the bottom of the reactor. Because of the high melting point of Li$_x$Si compared to Li metal, Li$_x$Si can withstand higher temperature in the reactor. Therefore, Li$_x$Si NPs were placed at the bottom of the reactor for 24 h, ensuring the formation of a crystalline and dense LiF coating.

Electrochemical testing. To investigate the electrochemical performances of coated and uncoated Li metal, symmetric type-2032 coin cells were assembled with two identical electrodes with 20 µL carbonate-based electrolyte (1M LiPF$_6$ in 1:1 EC/DEC, BASF). The impedance spectra were recorded over the frequency from 10^6 Hz to 0.1 Hz using a BioLogic VMP3 system. To prepare the LiF-Li$_x$Si electrodes, LiF-Li$_x$Si NPs, carbon black (Super P, TIMCAL, Switzerland), and polyvinylidenefluoride binder (PVDF, Kynar HSV 900) (65:20:15 by weight) were dispersed uniformly in anhydrous DOL (Sigma Aldrich) or anhydrous NMP (Sigma Aldrich) to form a slurry. The slurry was then drop casted onto a copper foil and dried under vacuum. The total mass loading of LiF-Li$_x$Si anode was ~2.0

mg/cm^2. For the fabrication of LFP cathode, a LFP slurry (LFP (MTI Inc):Super P:PVDF =70:20:10) was coated onto Al foil and dried under vacuum. For LTO anode, a LTO slurry (LTO (MTI Inc):Super P:PVDF=80:10:10) was coated onto Cu foil. The total mass loading was ~10 mg/cm^2. Coin cells were assembled using a Li metal foil as counter/reference electrode. Galvanostatic cycling of symmetric Li metal cells and LiF-Li$_x$Si cells was carried out on a MTI 8 Channel battery tester and a 96-channel battery tester (Arbin Instruments).

Fabrication and test of Li/polysulfides cells.

Preparation of polysulfide catholyte: Blank electrolyte was prepared by dissolving an appropriate amount of lithium bis-trifluoromethanesulphonylimide (1 M) in 1,2-dimethoxyethane (DME) and 1,3-dioxolane (DOL) (1:1 by volume). The polysulfide catholyte was prepared by chemically reacting sublimed sulfur and an appropriate amount of lithium sulfide (Li$_2$S) in the blank electrolyte to form Li$_2$S$_8$ (5 M sulfur) in the solution. The solution was then stirred at 60 ºC in an Ar-filled glove box overnight to produce a brownish-red Li$_2$S$_8$ catholyte solution.

Preparation of carbon nanofiber membrane: 200 mg of carbon nanofiber powder (Fisher Scientific) was dispersed in isopropyl alcohol (100 mL) by high-power ultrasonication for 0.5 h and vacuum filtered through a nylon membrane with a pore size of 0.44 μm. After washing with deionized water and ethanol, followed by drying at 50 ºC for 30 min, the carbon nanofiber membrane could be easily peeled from the filter surface and used as a freestanding current collector. The obtained carbon nanofiber membrane was then punched out into circular disks with 1.1 cm diameter (1 cm^2).

Electrochemical Measurements: 12.5 μL of Li$_2$S$_8$ catholyte was added into carbon nanofiber electrode, corresponding to a sulfur loading of 2 mg/cm^2. The Celgard 2400 separator was then placed on top of the electrode, followed by adding 30 μL of the blank electrolyte. Finally, the Li metal with or without LiF coating was placed on the separator as the anode. An Arbin battery cycler was used to

perform the galvanostatic cycling measurements at 1.7 - 2.8 V (*vs.* Li/Li$^+$) at room temperature. The current density set for tests was referred to the mass of sulfur in the cathode and was tested at C/10 for the first 2 times and C/5 for the following cycles.

Characterizations. TGA-MS analysis is performed under N_2 atmosphere at a heating rate of 5 ºC/min, tracing the signals of $C_xH_yF_z$ (x, y, z=0, 1, 2…) fragments with mass-to-charge ratio less than 138. The pristine and cycled Li metal electrodes were cross-sectioned with a Ga$^+$ ion beam and observed with the electron beam on a FEI Helios NanoLab 600i DualBeam FIB/SEM. SEM images were acquired using a FEI XL30 Sirion SEM. TEM images were taken on a FEI Tecnai G2 F20 X-TWIN TEM at an acceleration voltage of 200 kV and FEI Titan 80–300 environmental TEM at an acceleration voltage of 300 kV. Powder X-ray diffraction was performed on a PANalyticalX'Pert with Ni-filtered Cu Kα radiation. The XRD samples were sealed with Kapton tape (DuPont) to eliminate possible side reactions in the air. XPS analysis was performed on PHI Versa Probe 5000, Physical Electronics, USA. For sputter depth profiling, Ar$^+$ ions of 1 keV energy at a scan size of 2 mm×2 mm was utilized.

Supporting Figures
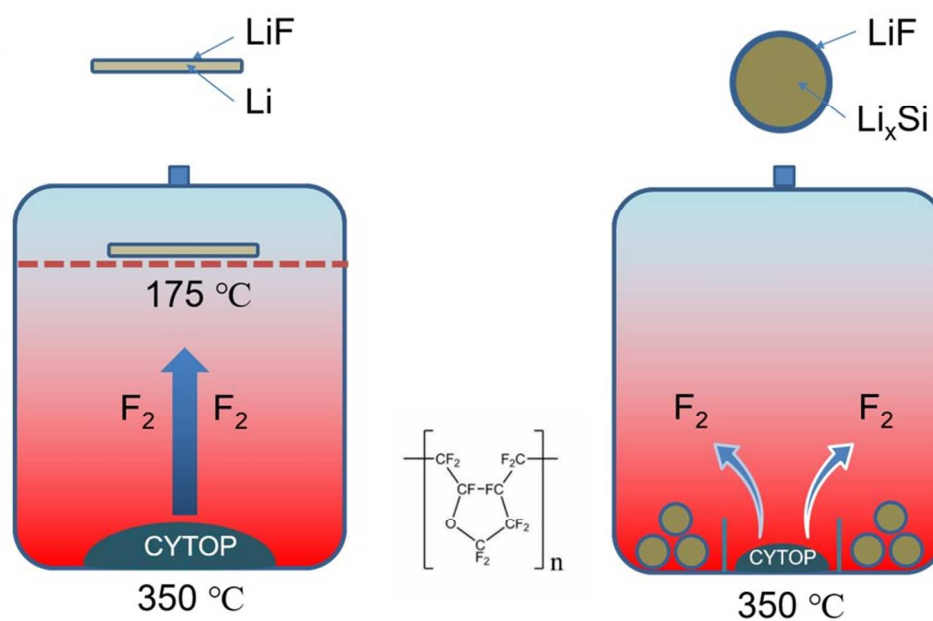
Supplementary Figure 1. Schematic of the fluorination reactors for lithium metal and prelithiated silicon anodes. Upon heating, the fluoropolymer, CYTOP, gradually decomposes and releases fluorine gas, which react with the surface of Li metal and Li_xSi NPs to form a uniform and compact LiF layer.
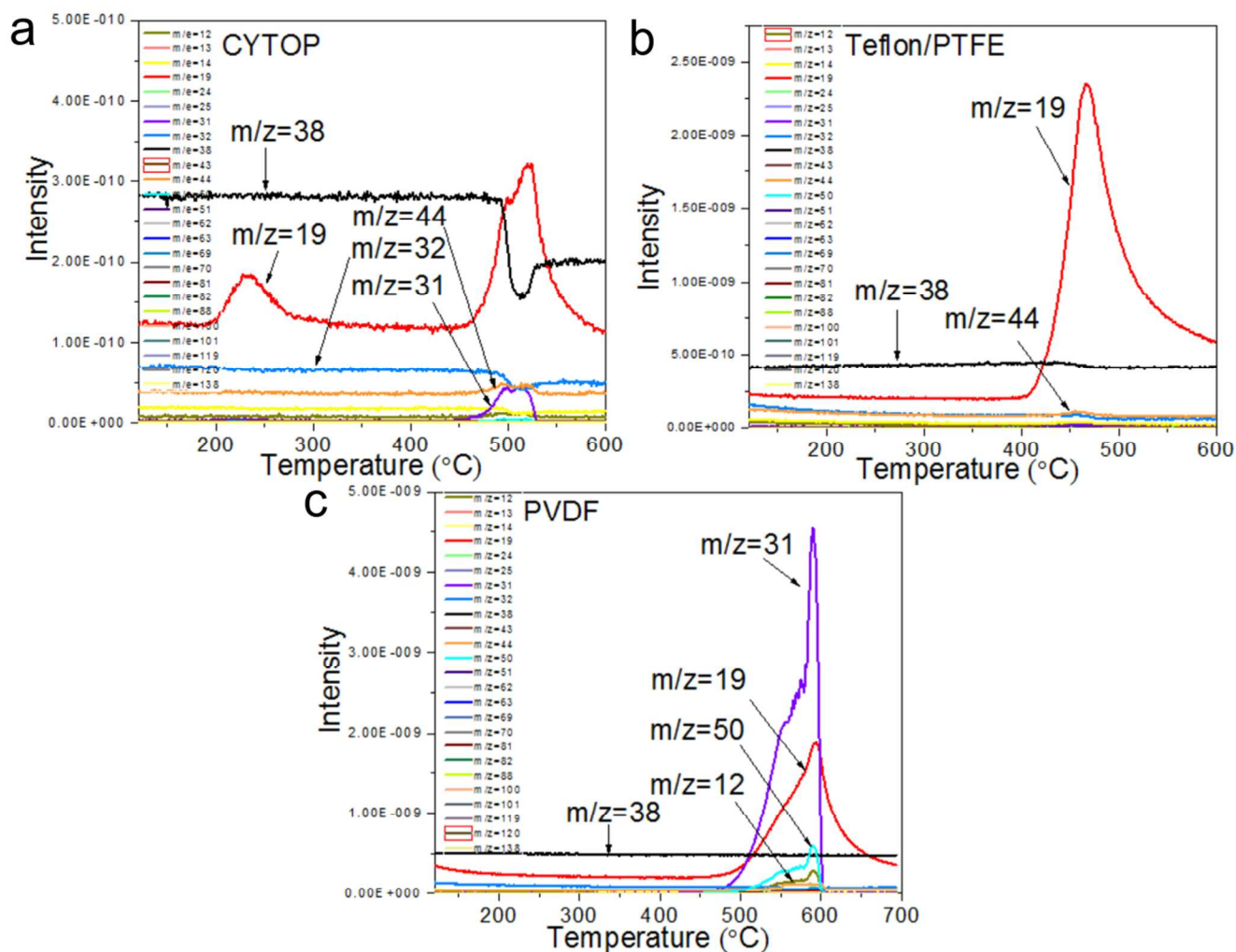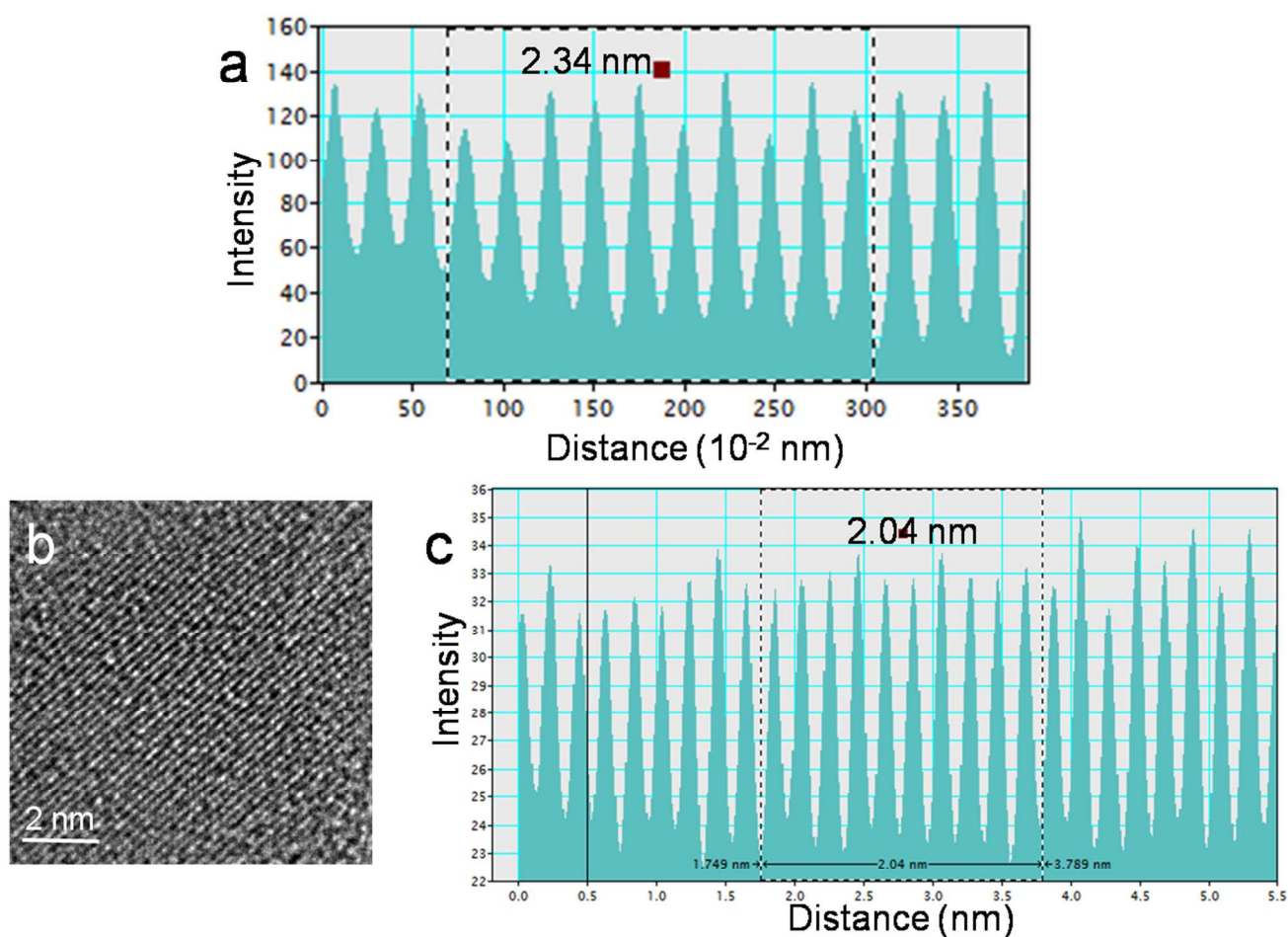
**Supplementary Figure 2.** TGA-MS analysis of **(a)** CYTOP, **(b)** Teflon, and **(c)** PVDF.
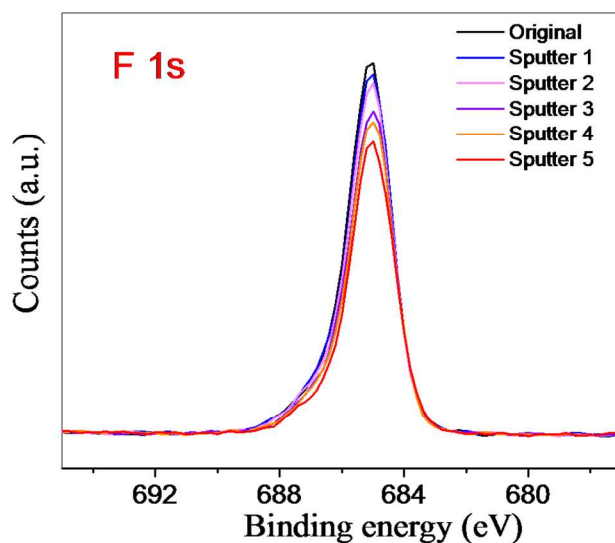
Supplementary Figure 3. The sputtering depth profile of F 1s performed on LiF-coated Li metal.
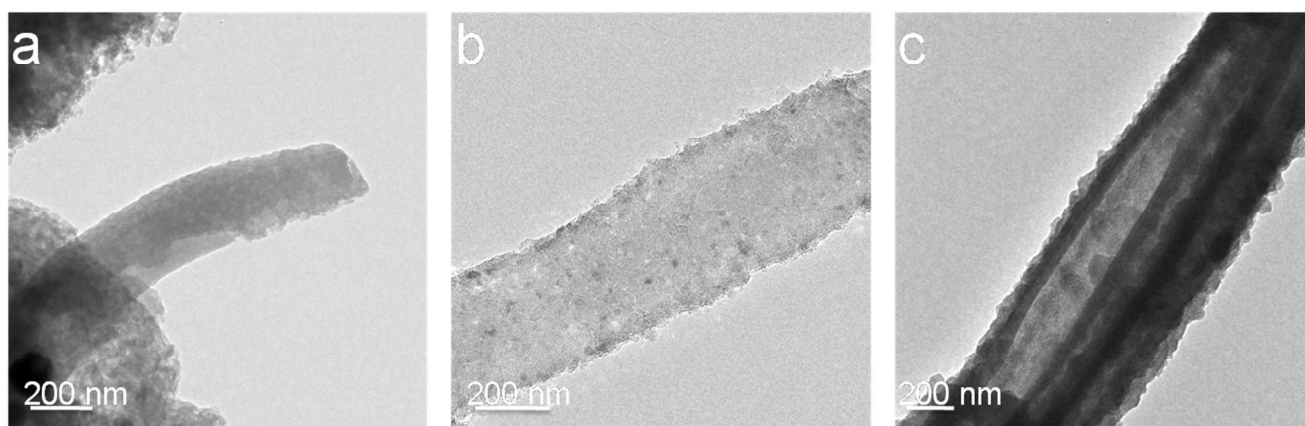
Supplementary Figure 4. (a) TEM image of uncoated Li metal. TEM images of Li metal treated in fluorination reactor for **(b)** 1h and **(c)** 6 h.


Supplementary Figure 5. (a) The intensity plot shows that ten layers span a distance of 2.34 nm (average plane spacing: 0.234 nm), corresponding to the (111) plane of LiF. **(b)** High-resolution TEM image shows (200) lattice plane of LiF nanocrystal with **(c)** plane spacing of 0.204 nm.
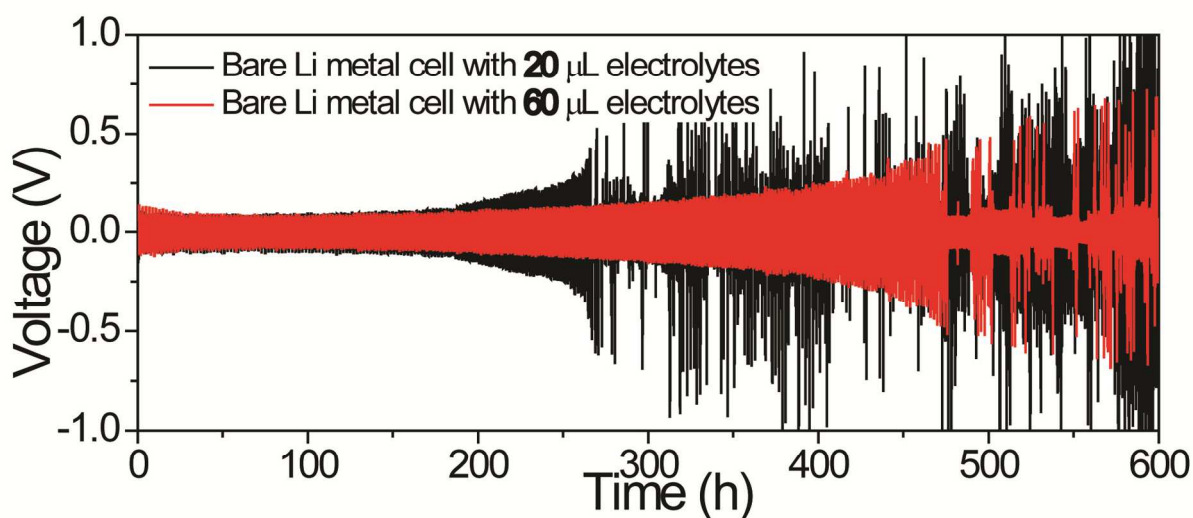
Supplementary Figure 6. Cycling stability of the bare Li metal symmetric cells with 20 µL (black) and 60 µL (red) carbonate electrolytes at a current density of 1 mA/cm^2.
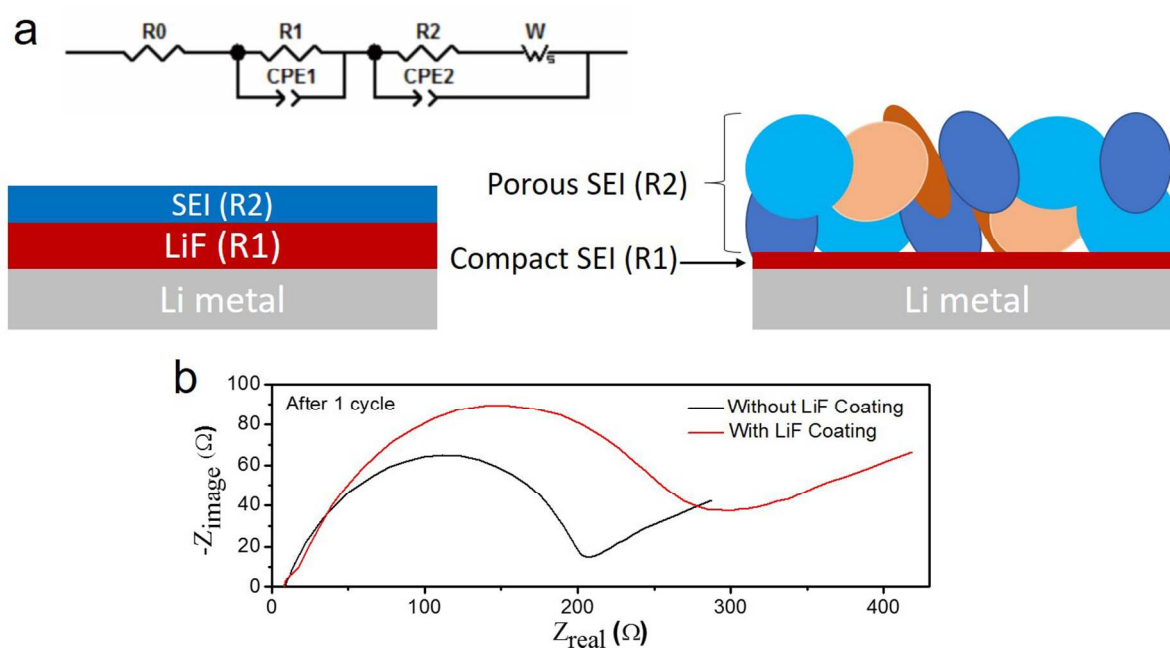

Supplementary Figure 7. (a) The equivalent circuit and the schematic of interfacial layers on LiF-coated Li metal and bare Li metal anodes. **(b)** Nyquist plot of the impedance spectra of the symmetrical LiF-coated Li metal and bare Li metal cells after first cycle at a current density of 1 mA/cm^2.
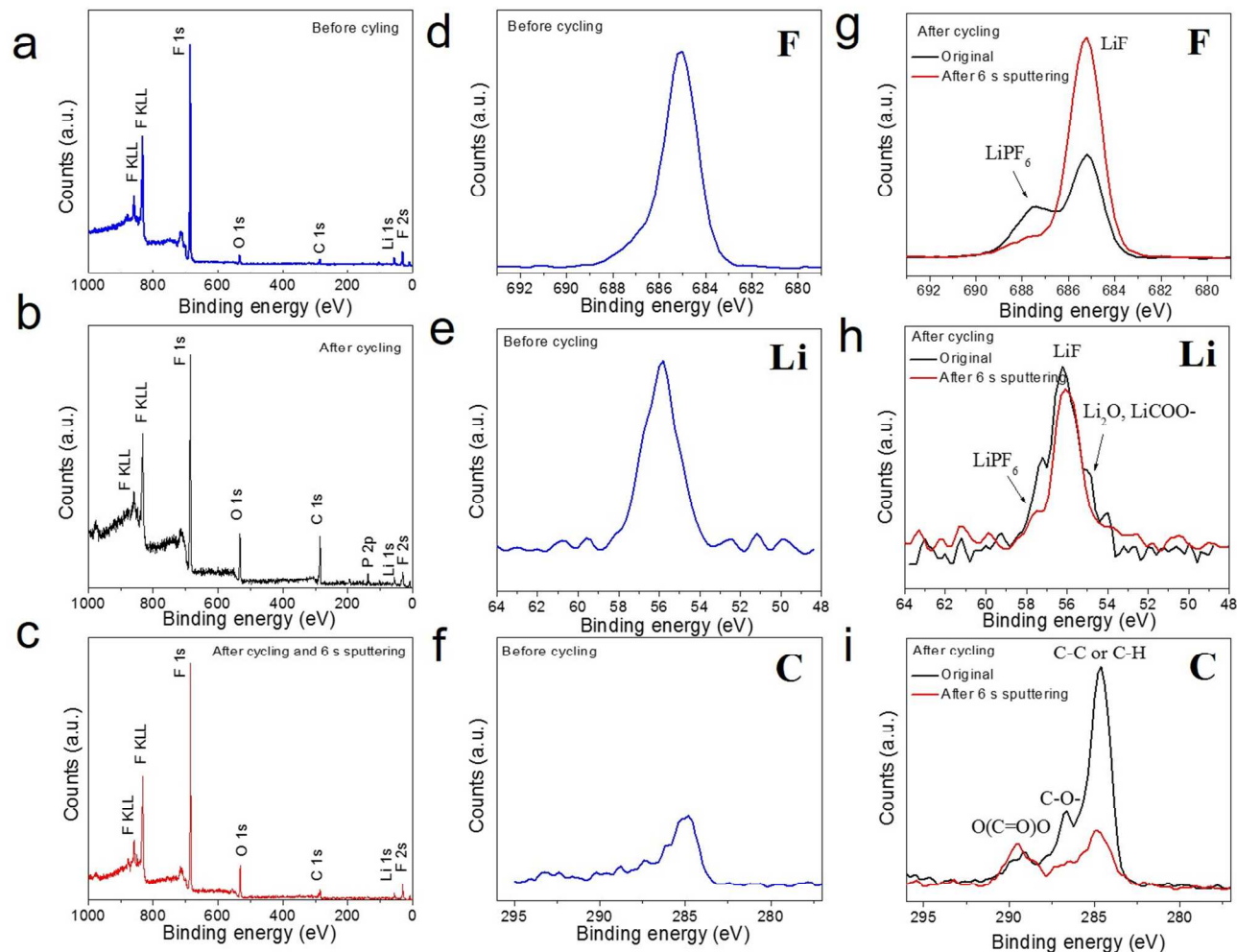
Supplementary Figure 8. (a) XPS spectrum of the LiF-coated Li metal. XPS spectra **(b)** before and **(c)** after 6 s sputtering for LiF-coated Li metal cycled in the symmetric cell for 300 times at the current density of 1 mA/cm^2. High-resolution XPS spectra of **(d)** F1s, **(e)** Li 1s, and **(f)** C 1s of the LiF-coated Li metal. High-resolution XPS spectra of **(g)** F1s, **(h)** Li 1s and **(i)** C 1s before and after 6 s sputtering for the LiF-coated Li metal cycled in the symmetric cell for 300 times at the current density of 1 mA/cm^2. For sputter depth profiling, Ar$^+$ ions of 1 keV energy at a scan size of 2 mm×2 mm and a 6 s sputtering time was utilized.
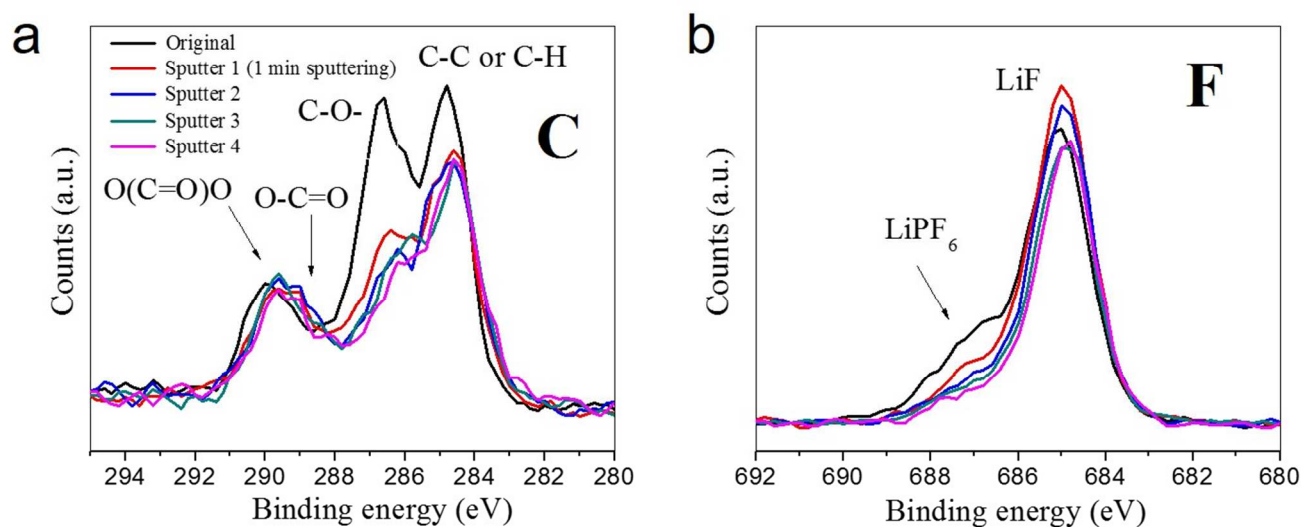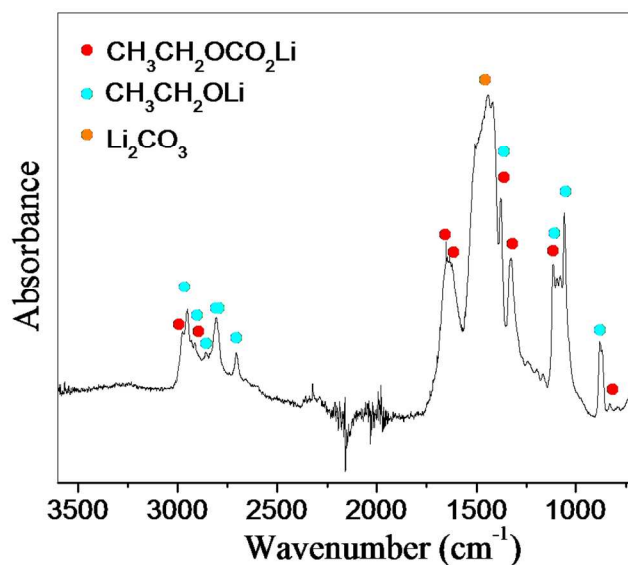
Supplementary Figure 9. The sputtering depth profile of **(a)** C1s and **(b)** F 1s spectra performed on bare Li metal cycled in the electrolyte of 1.0 M $LiPF_6$ in 1:1 v/v EC/DEC for 50 times. For sputter depth profiling, Ar^+ ions of 1 keV energy at a scan size of 2 mm×2 mm and a 1 min sputter interval was utilized.
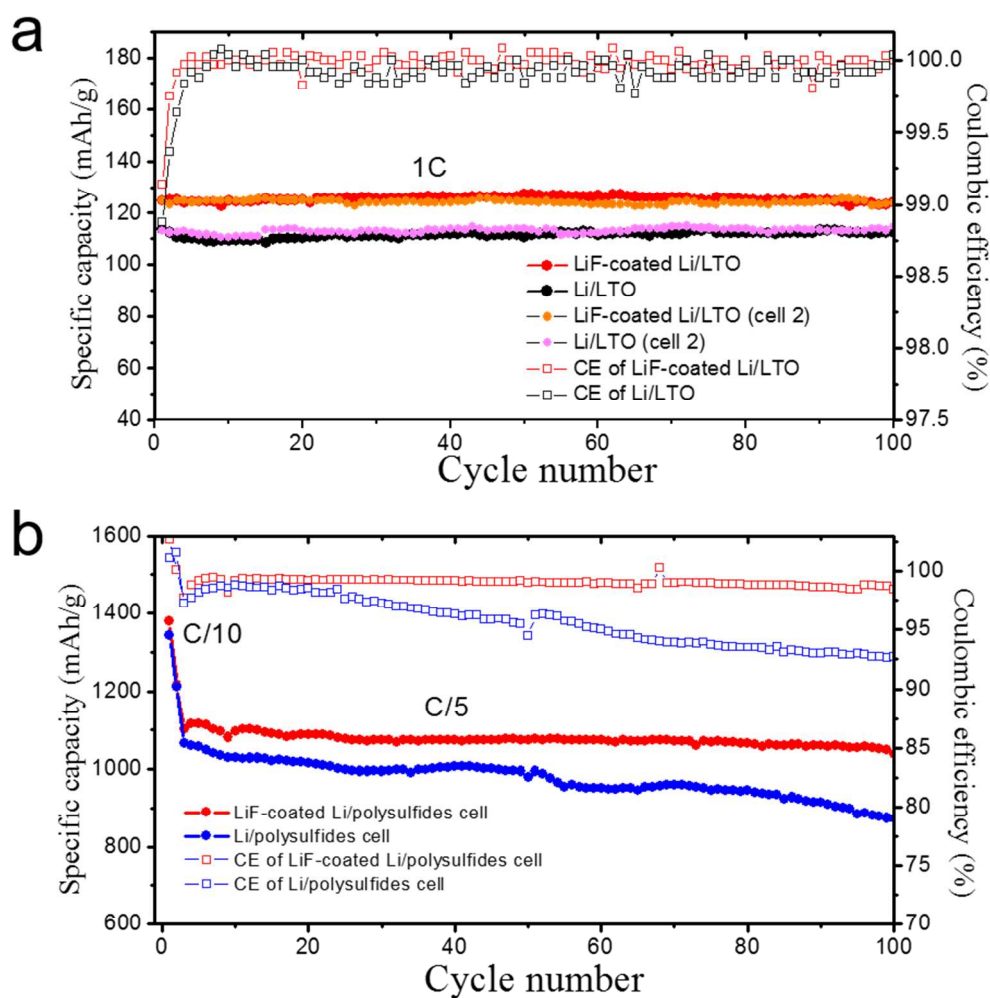
Supplementary Figure 10. (a) Cycling performance and Coulombic efficiency (CE) of LiF-coated Li metal/Li$_4$Ti$_5$O$_{12}$ (LTO) (red) and bare Li metal/LTO (LTO:Super P:PVDF=8:1:1 by weight) (black) cells at the rate of 1 C. The capacity and rate are both based on the mass of LTO. The cycling data of two cells are shown for each cell configuration. **(b)** Cycling performance of LiF-coated Li/polysulfides (red) and Li/polysulfides (blue) cells at C/10 for the first 2 cycles and C/5 for the following cycles (1C=1.67 A/g of S. The capacity is based on the mass of S in the cathode). The Coulombic efficiency is plotted on the secondary y-axis.
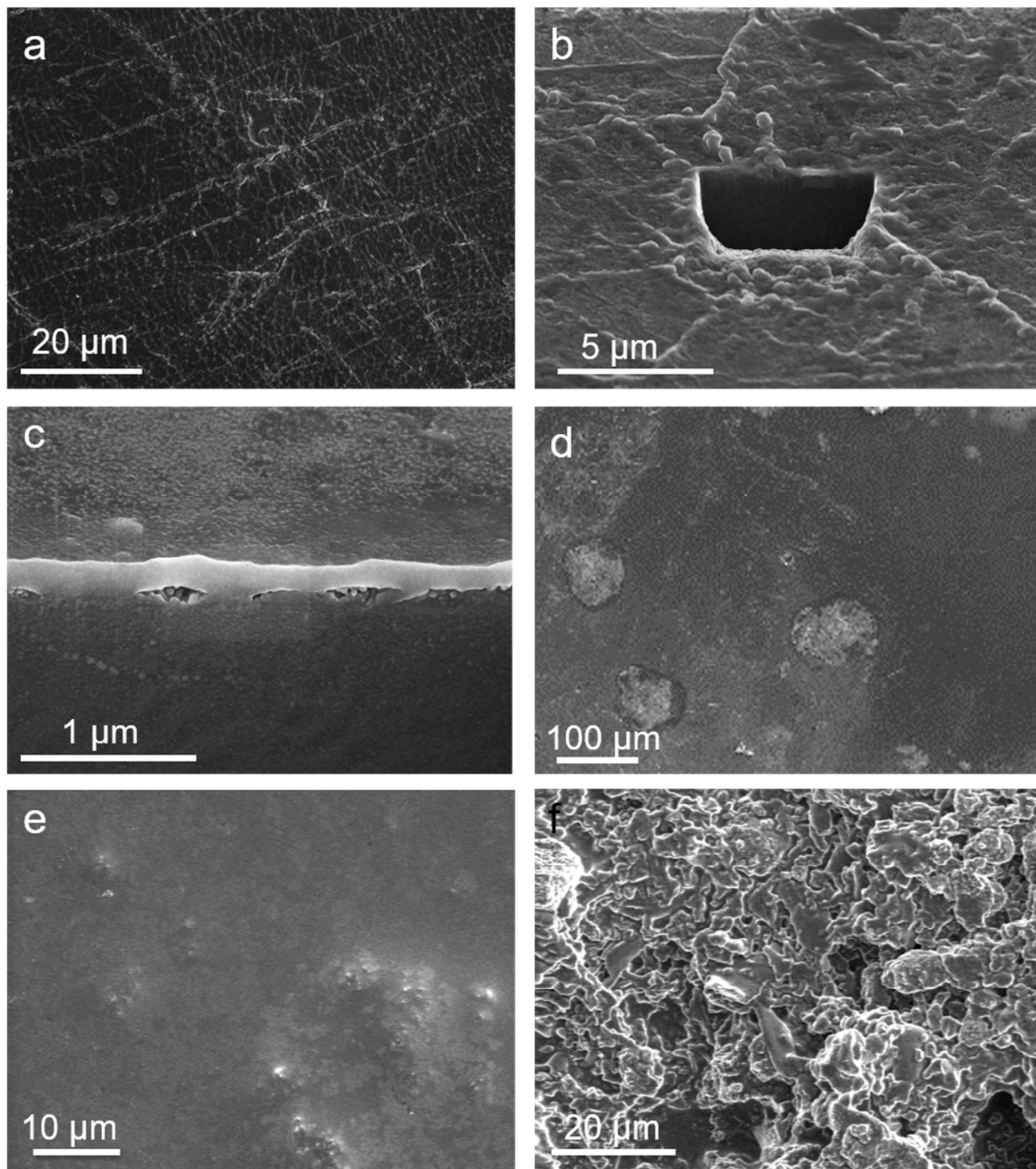
Supplementary Figure 11. FIB-SEM images of LiF-coated Li metal (12 h fluorination treatment) after 50 cycles **(a)** before and **(b)** after Ga$^+$ ion beam cutting. **(c)** FIB-SEM image of LiF-coated Li metal with 6 h fluorination treatment. **(d)** SEM image of LiF-coated Li metal (6 h fluorination treatment) after 50 cycles of stripping/plating in the symmetric cell with the electrolyte of EC/DEC. SEM images of Li metal anodes covered with ball-milled LiF NPs **(e)** before and **(f)** after cycled in the symmetric cell for only 10 times.
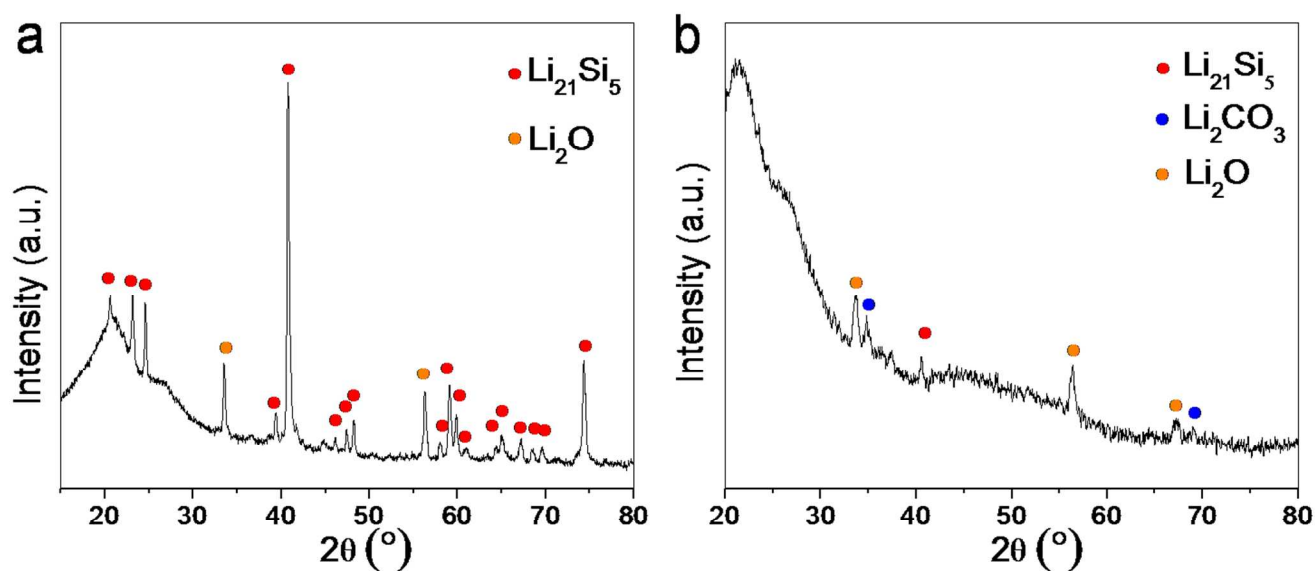

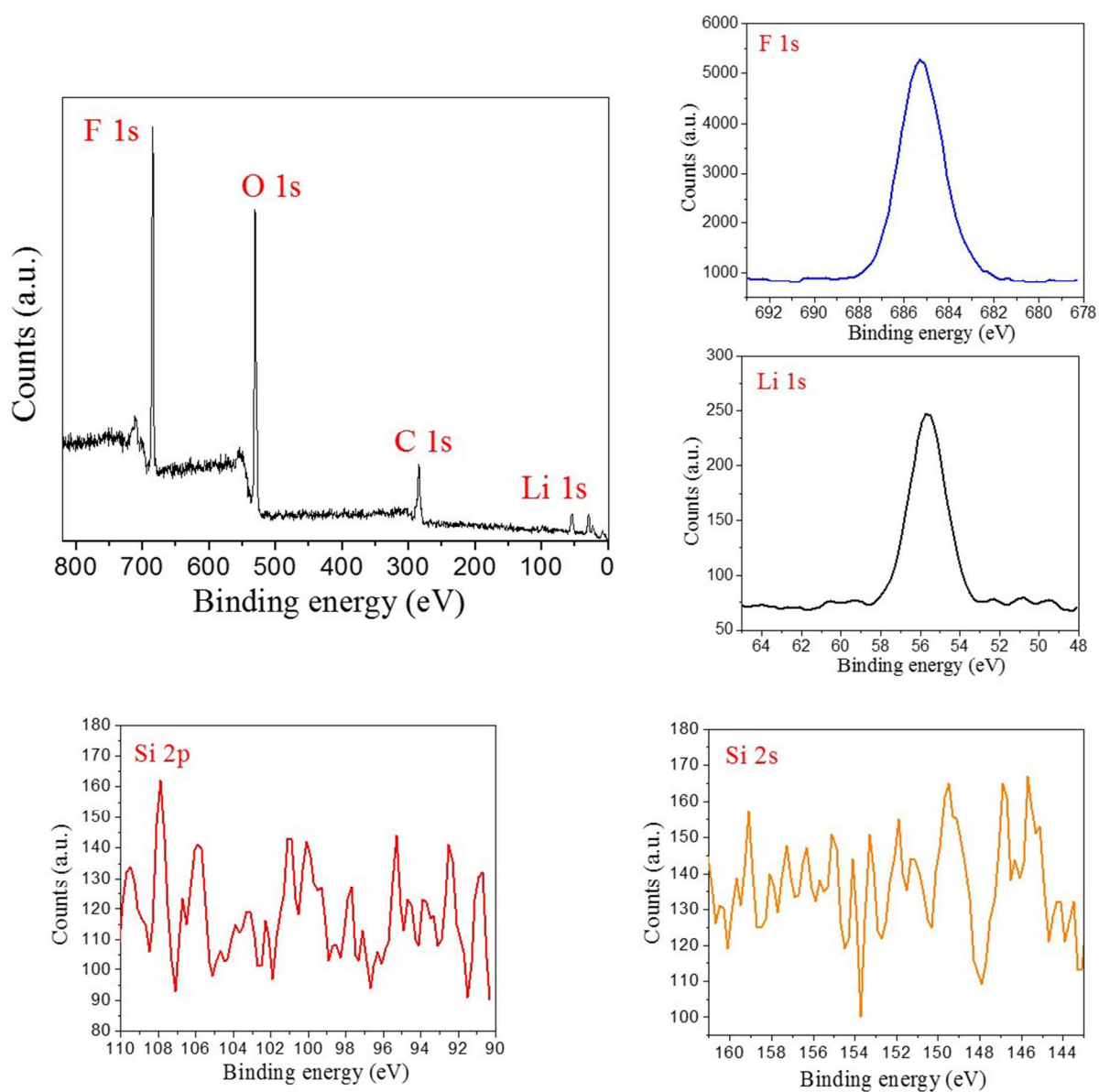**Supplementary Figure 12.** FT-IR analysis of bare Li metal soaked in DEC for 6 h.
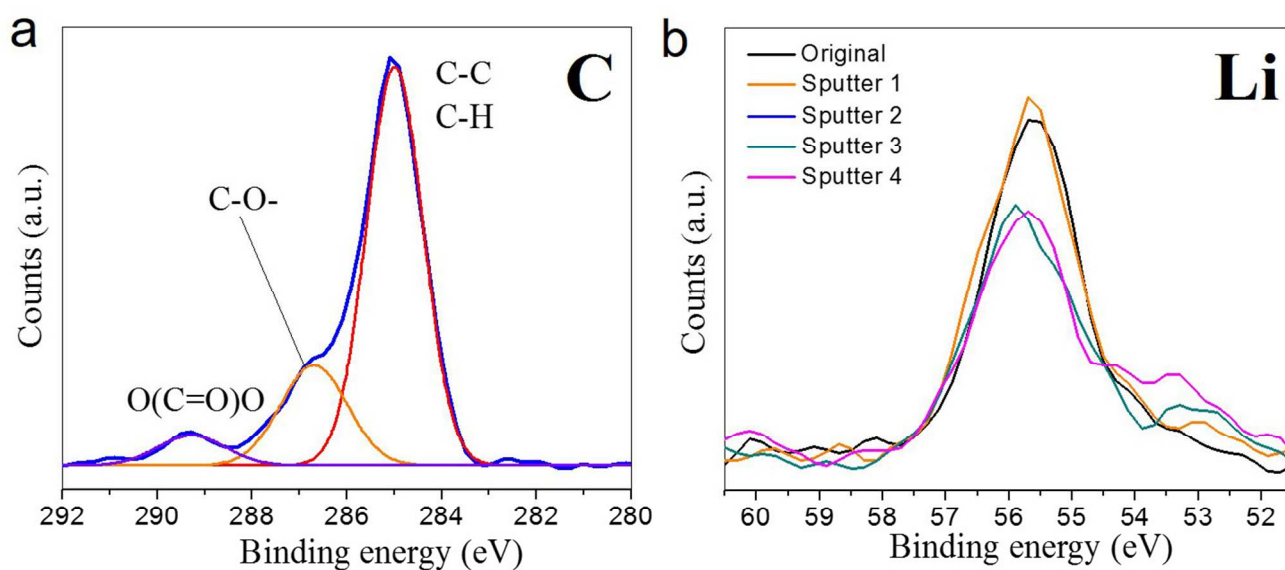
Supplementary Figure 13. (a) High-resolution XPS spectrum of C1s and **(b)** sputtering depth profile of Li 1s performed on the bare Li metal operated in electrolytes consisting of 1.0 M LiPF$_6$ in 1:1 v/v EC/DEC with 10 vol% FEC for one cycle.
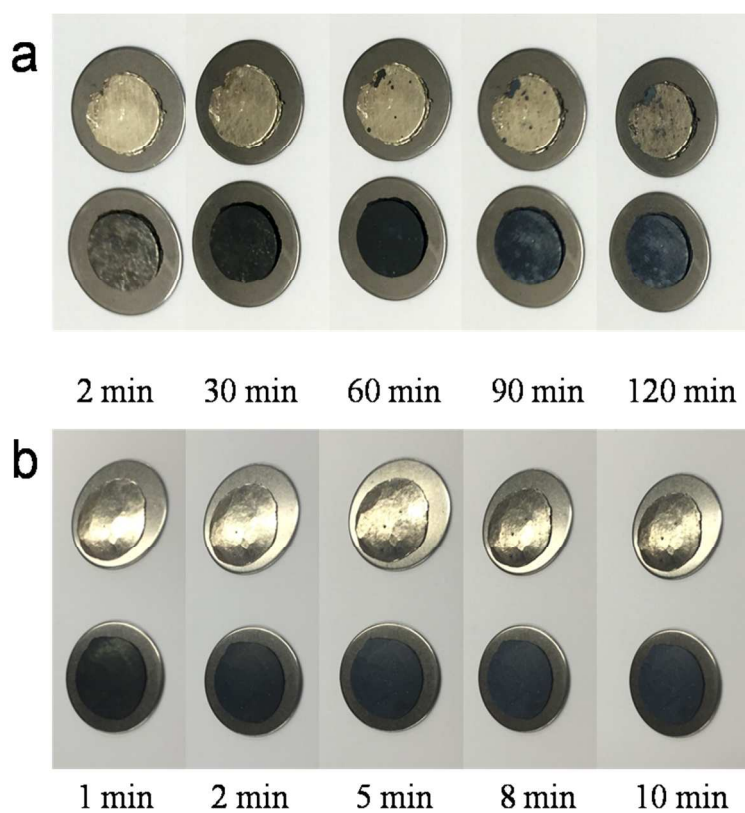
Supplementary Figure 14. (a) Photographs of coated (upper) and uncoated Li metal (bottom) exposed in the air with humidity level of 20% RH for 2 h. **(b)** Photographs of coated (upper) and uncoated Li metal (bottom) exposed in the air with humidity level of 40% RH for 10 min.
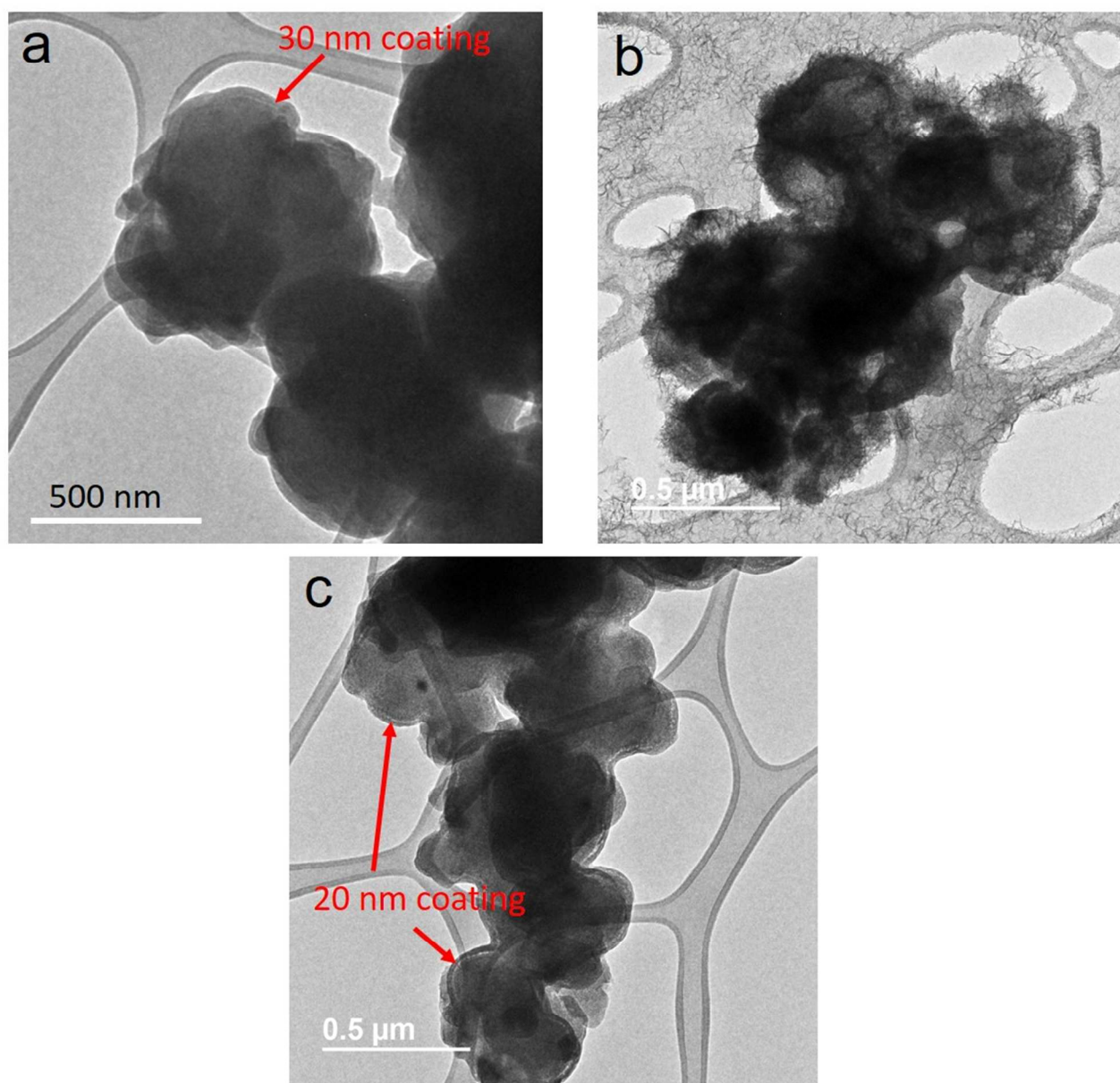

Supplementary Figure 15. (a) XRD pattern of the metallurgically synthesized Li_xSi NPs. **(b)** XRD pattern of uncoated Li_xSi NPs after soaked in NMP for 6h.
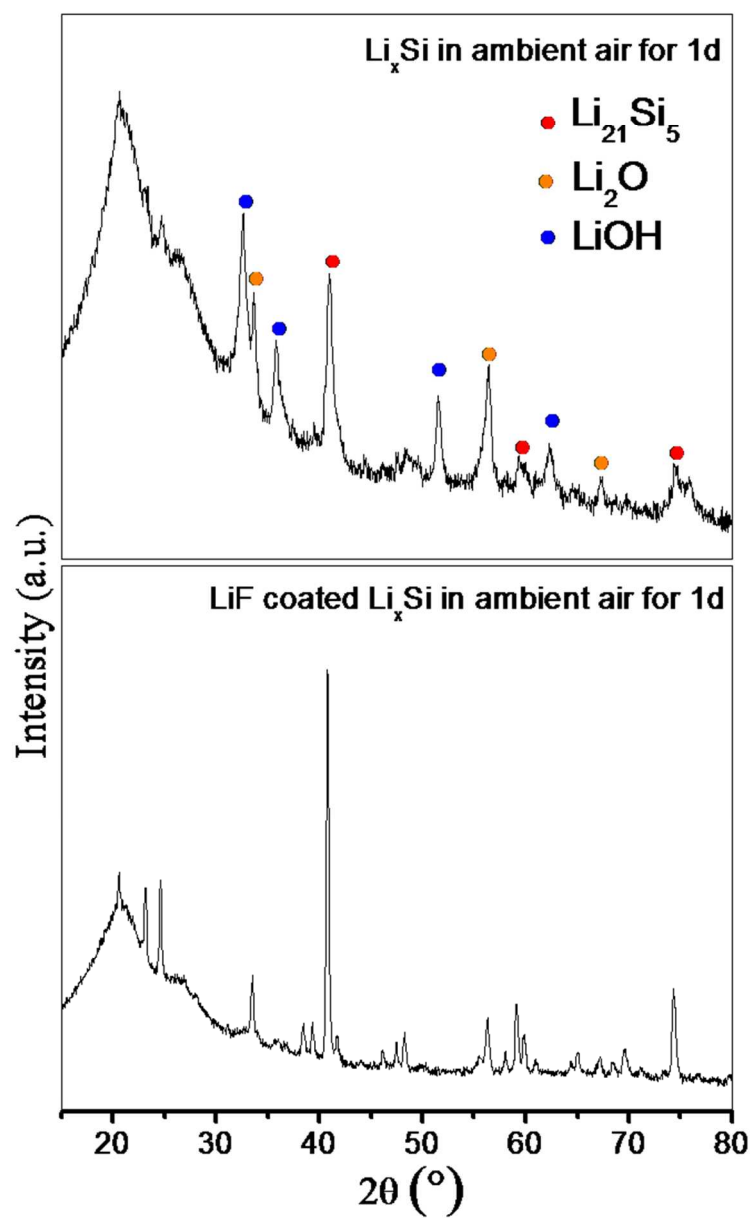
Supplementary Figure 16. XPS analysis of the LiF-coated Li$_x$Si NPs and the corresponding high resolution XPS spectra of Li 1s, F1s, Si 2p and Si 2s.
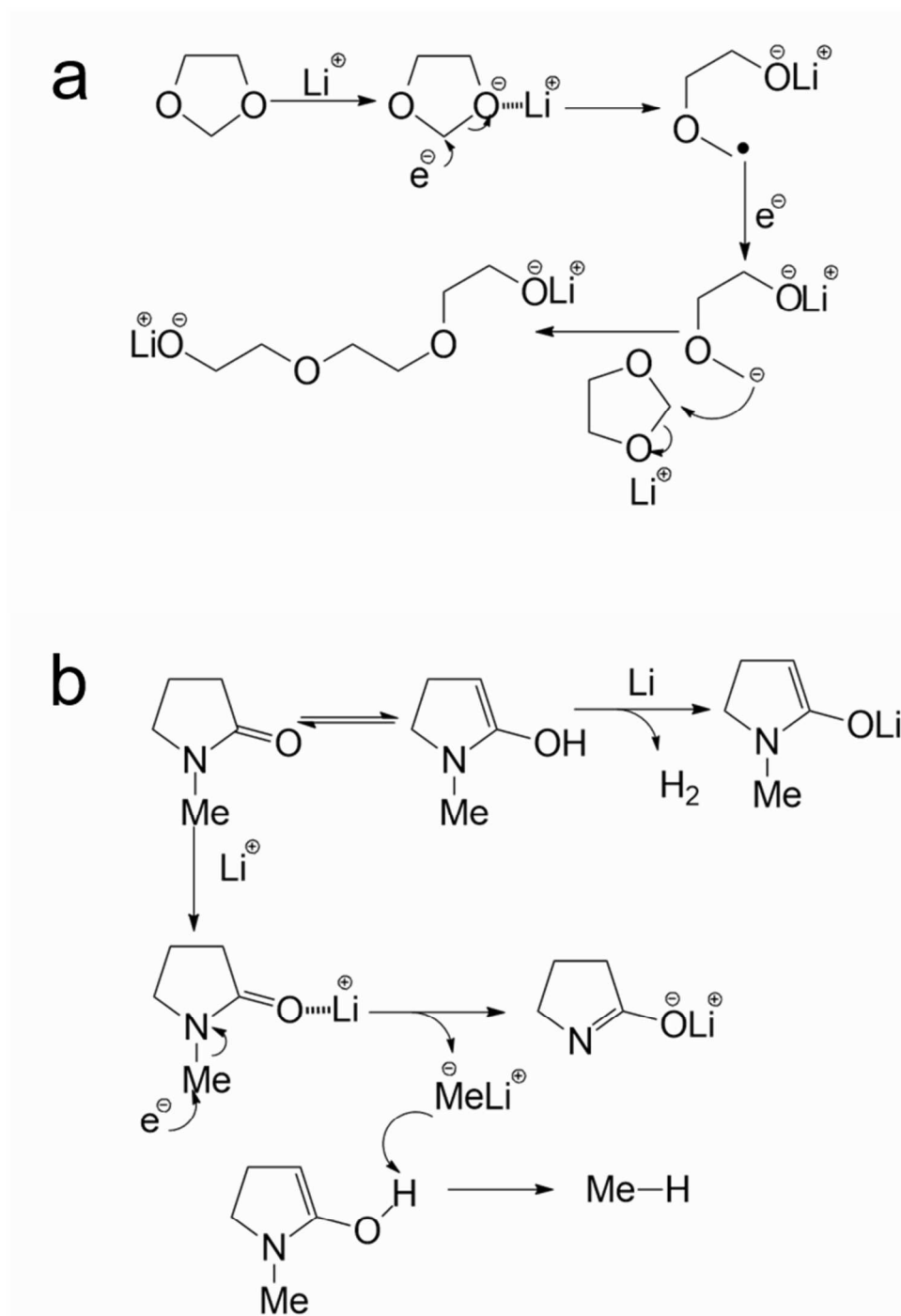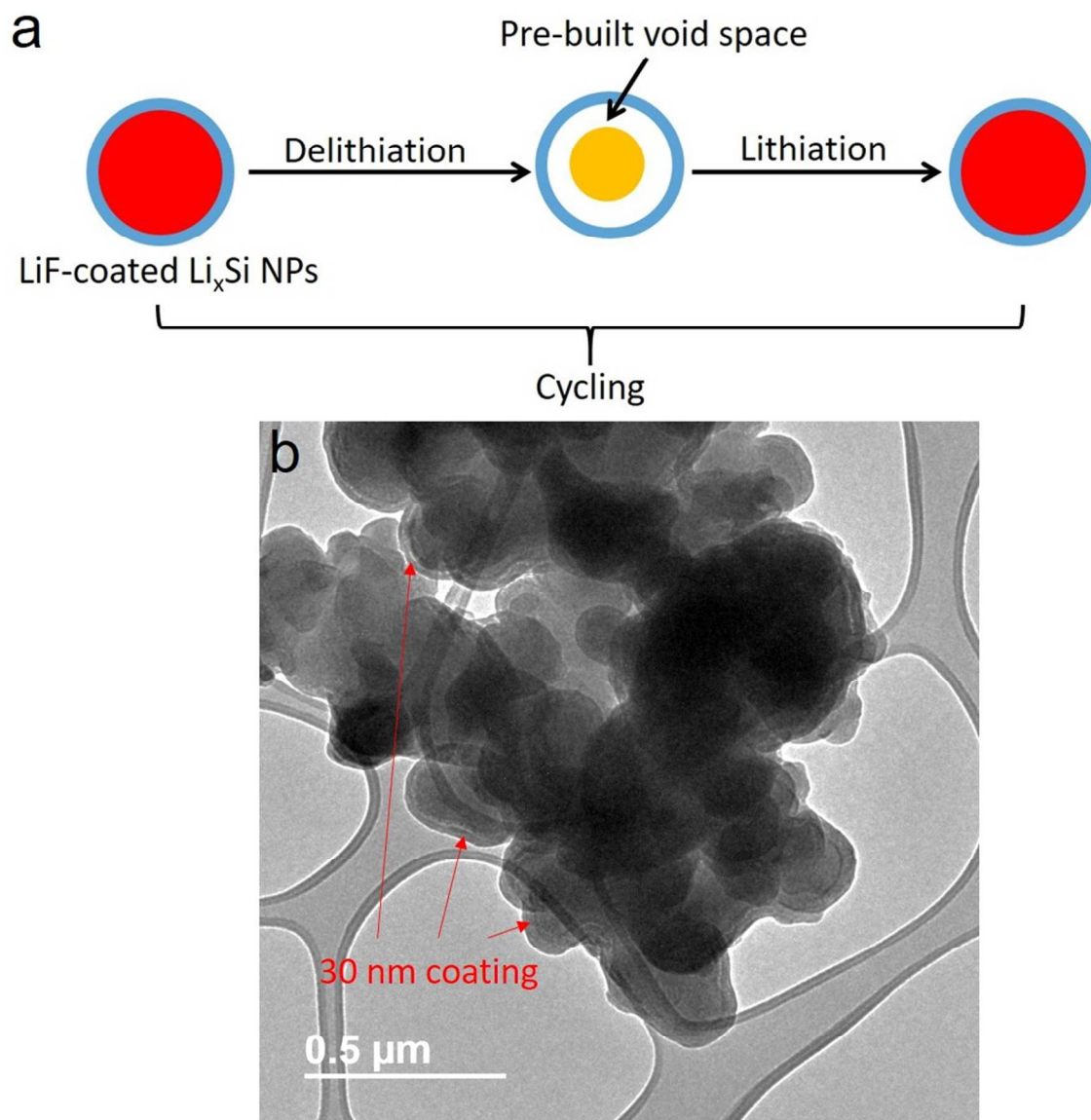
Supplementary Figure 17. The reaction mechanisms with **(a)** DOL **(b)** NMP.

Supplementary Figure 18. TEM images of bare Li$_x$Si NPs soaked in **(a)** DOL and **(b)** NMP for 0.5 h. **(c)** TEM image of LiF-coated Li$_x$Si NPs soaked in NMP for 0.5 h.

Supplementary Figure 19. XRD patterns of uncoated (upper) and coated (bottom) Li_xSi NPs exposed to the ambient air (~40% RH) for one day.

Supplementary Figure 20. (a) A schematic illustrates the structures of LiF-coated Li$_x$Si NPs before and during cycling. **(b)** TEM image of LiF-coated Li$_x$Si NPs cycled in the cell for 300 times and stopped at the lithiated state. To avoid the disturbance of the PVDF binder and conductive carbon, the LiF-coated Li$_x$Si NPs were dispersed in cyclohexane and then drop-casted on copper foil.
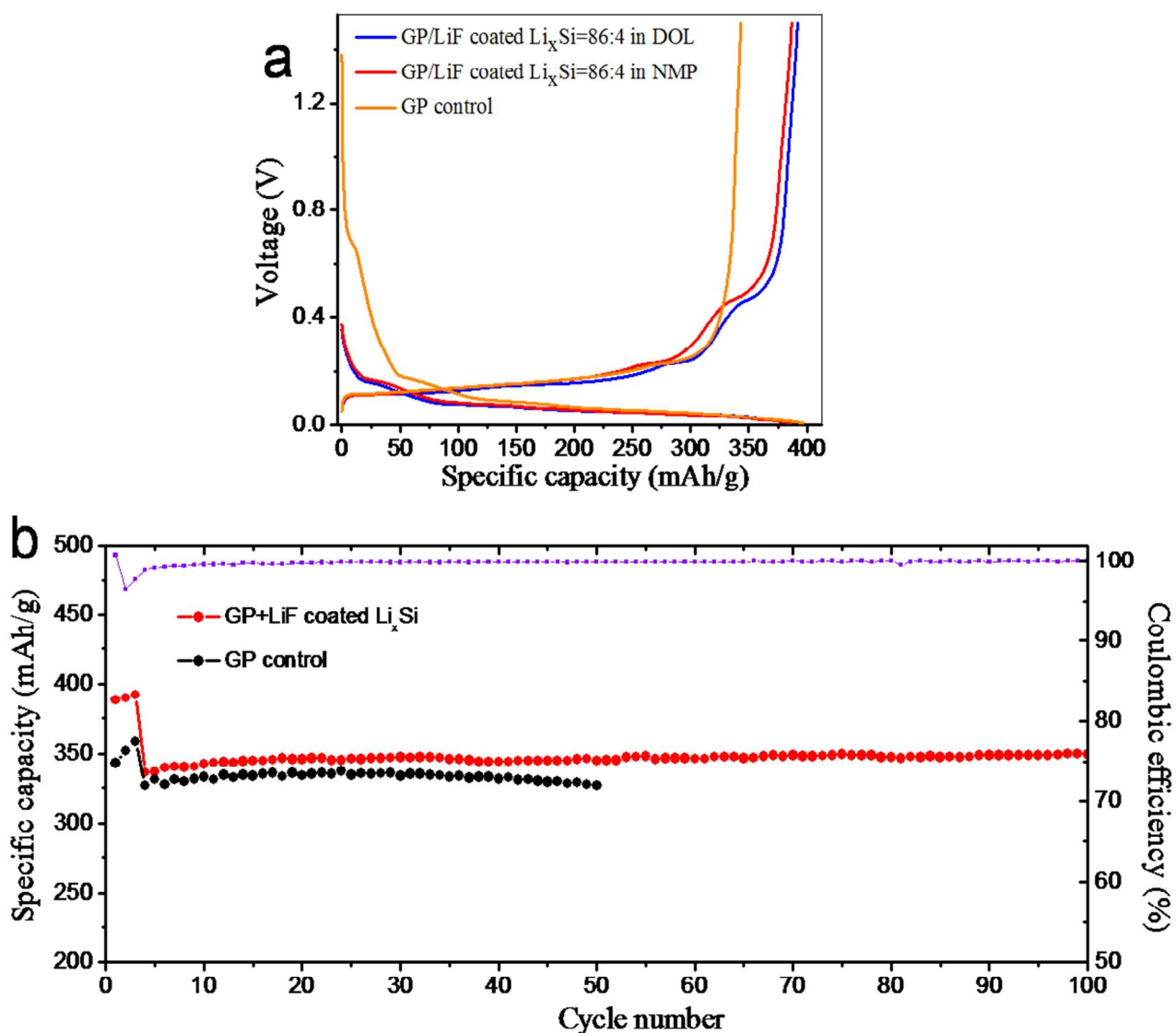
Supplementary Figure 21. (a) First-cycle voltage profiles of graphite/LiF-coated Li$_x$Si composite (86:4 w/w), using different solvents to prepare the slurry. **(b)** Cycling performance of graphite/LiF-coated Li$_x$Si composite and graphite control cells at C/20 for the first three cycles and C/5 for the following cycles (1 C = 0.372 A/g. The capacity is based on the mass of graphite and Si in LiF-coated Li$_x$Si NPs. NMP is used as the slurry solvent). The purple line is the Coulombic efficiency of the graphite/LiF-coated Li$_x$Si composite.